JACS
JOURNAL OF THE AMERICAN CHEMICAL SOCIETY

Communication

pubs.acs.org/JACS

Polymer-Stabilized Perfluorobutane Nanodroplets for Ultrasound Imaging Agents

Yuran Huang,[†] Alexander M. Vezeridis,[‡] James Wang,[§] Zhao Wang,[§] Matthew Thompson,[§] Robert F. Mattrey,[‡] and Nathan C. Gianneschi*[,†,§]

[†]Materials Science & Engineering Program, [‡]Department of Radiology, and [§]Department of Chemistry & Biochemistry, University of California—San Diego, La Jolla, California 92093, United States

Supporting Information

ABSTRACT: In this paper, we describe a method for the stabilization of low-boiling point (low-bp) perfluorocarbons (PFCs) at physiological temperatures by an amphiphilic triblock copolymer which can emulsify PFCs and be cross-linked. After UV-induced thiol−ene cross-linking, the core of the PFC emulsion remains in liquid form even at temperatures exceeding their boiling points. Critically, the formulation permits vaporization at rarefactional pressures relevant for clinical ultrasound.

Ultrasound imaging is one of the most widely used diagnostic imaging modalities, because it is noninvasive in nature, utilizes nonionizing radiation, is relatively low cost, is portable, and lends real-time visualization.[1,2] Contrast in clinical ultrasound is based on the variation of acoustic impedance from various tissues, which is relatively low compared to other imaging techniques.[3] Air microbubbles can greatly enhance the contrast but suffer rapid disappearance resulting from the combined effects of high solubility in aqueous solution, high Laplace pressure in biological fluids, and microbubble trapping in the lungs.[4,5] Therefore, perfluorocarbons (PFCs) have been utilized as the gaseous core of microbubbles because of their insolubility in biological fluids leading to a decreased bulk transfer and an increased half-life.[6,7] Although liquid PFC microdroplets are effective ultrasound contrast agents at high doses,[8,9] gas phase PFC microbubbles are far more effective requiring 1/30th the dose on grayscale ultrasound imaging[10] and produce even higher image contrast with nonlinear imaging.[11] Therefore, there would be a distinct advantage if liquid PFCs could be formulated as microdroplets, able to be activated acoustically *in vivo* using an externally applied ultrasound pulse to form a gaseous microbubble. This approach is known as acoustic droplet vaporization (ADV). Wherein, the phase transition of microdroplet-to-microbubble dramatically increases acoustic backscatter resulting in the generation of ultrasound contrast.[12]

The boiling points (bp) of PFCs vary widely depending on carbon content and branching, from −183.6 °C to +142 °C or higher. PFCs with boiling points below physiological temperatures (low-bp PFCs) can be vaporized at acoustic pressures accessible to clinically diagnostic ultrasound machines, but their inherent instability at those temperatures limits their utility in clinical applications. For those PFCs with boiling points higher than physiological temperatures (high-bp PFCs), rarefactional pressures allowed by clinical ultrasound are not able to trigger their liquid-to-gas phase transition. Therefore, high intensity focused ultrasound (HIFU) is used to assist this process. Unfortunately, these higher energies are associated with a higher risk of tissue damage.[13,14] Therefore, finding the PFC with a correct balance between spontaneous vaporization and stability for ADV applications is an ongoing and important challenge. In short, one desires a formulation that is stable at physiological temperatures but can transit to microbubbles at low ultrasound energy.

Various nanocarriers have been employed for PFC-based ultrasound contrast agents, including liposomes,[15,16] polymeric nanoparticles,[17,18] protein,[19] and inorganic nanoparticles.[20−22] These strategies generally involve building a functionalized shell around the PFC core to improve stability by reducing surface tension, to provide a diffusion barrier, and in some cases a functionalizable surface for targeting.[23] Nanocarrier-based stabilization of PFCs has largely been limited to high-bp PFCs, likely because they are easily stored and easily handled.[24,25] In the case of low-bp PFCs, polymeric encapsulating shells provide a route to increasing the Laplace pressure and enhancing the stability of the liquid droplets.[26,27] However, polymer-based shells have been obtained by self-assembly of amphiphiles at the interface, allowing PFCs to undergo bulk transfer out of the droplet.[28] Cross-linking the polymeric shell provides an option for stabilization of the polymeric network and to prevent bulk transfer of PFCs. A DNA-based cross-linking strategy has been used to hinder nonlinear oscillation of microbubbles in response to ultrasound stimulus.[29] Amino groups on a polymer scaffold were also used as functional groups for reaction with with glutaraldehyde to form cross-linked shells, but the process is slow, requiring at least 1 day to cross-link, making the preparation difficult to deploy when using low boiling point PFCs.[30]

Considering the volatility of low-bp PFCs, we envisioned a simple, fast, robust strategy involving amphiphile assembly at the interface, followed by a fast, highly efficient cross-linking reaction capable of working at low temperatures for stabilizing the low-bp PFC microdroplets. We reasoned that UV-induced thiol−ene click chemistry had potential in this application given the ease of implementation, high yield at low temperatures, and rapid reaction rates.[31]

To enhance the stability of low-bp PFC droplets, and eventually move toward diagnostic ultrasound contrast enhancement, we designed a triblock copolymer system synthesized by

Received: August 22, 2016
Published: December 29, 2016

DOI: 10.1021/jacs.6b08800
J. Am. Chem. Soc. 2017, 139, 15−18

ring opening metathesis polymerization (ROMP),[32−34] consisting of a fluorinated block for emulsification of PFCs,[35] an alkene-modified block for secondary thiol−ene cross-linking under UV radiation, and an oligoethylene glycol hydrophilic block (Figure 1). The strategy was to stabilize a low-bp PFC emulsion at

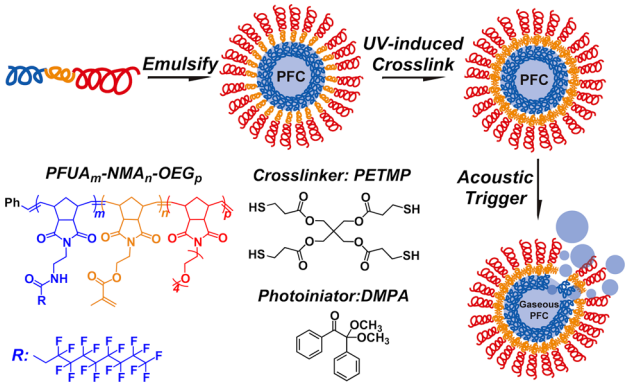

Figure 1. Preparation and acoustic droplet vaporization (ADV) of low-bp PFC emulsions stabilized by thiol−ene cross-linked ROMP block copolymers (PFUA$_m$-NMA$_n$-OEG$_p$) generated from monomers with side chains: perfluorundecanoic acid (blue, PFUA), methacrylic acid (yellow, NMA) and amino-modified oligoethylene glycol (red, OEG).

physiological temperatures following UV-induced thiol−ene cross-linking, while allowing a liquid-to-gas phase transition using clinical ultrasound systems.

A fluorinated monomer, for the first block, was prepared consisting of perfluoroundecanoic acid (PFUA) (Figures S1−S3). An alkene-modified monomer for UV-induced cross-linking was prepared consisting of a methacrylic acid (NMA) moeity (Figures S4−S5). A hydrophilic monomer was prepared based on an oligo(ethylene glycol) (OEG) functionality. To facilitate cross-linking, a thiol-based cross-linker, pentaerythritol tetra(3-mercapto-propionate) (PETMP), and a photoinitiator, 2,2-dimethoxy-2-phenylacetophenone (DMPA), were added to emulsions at low temperature (Figures 1 and S6).

Triblock copolymers of the type, PFUA$_m$-NMA$_n$-OEG$_p$, with varying block sizes were synthesized for exploration of optimal material properties (Figure S7). Ultimately, PFUA$_5$-NMA$_{10}$-OEG$_{32}$ was chosen to stabilize three kinds of PFCs including high-bp perfluorohexane (PFH, bp = 56 °C), low-bp perfluoropentane (PFP, bp = 29 °C,) and perfluorobutane (PFB, bp = −1.7 °C) (Figure S8). Complete reaction of the olefins and UV-induced cross-linking among this type of polymer were confirmed by ^{1}H NMR and size-exclusion chromatgraphy (Figures S9−S11). The UV-induced thiol−ene click reaction was confirmed as being capable of cross-linking the triblock copolymer at the low temperatures needed to generate stabilized emulsions in the presence of PFCs.

For optimization of the emulsification of PFCs, PFH (bp 56 °C) was first encapsulated in PFUA$_5$-NMA$_{10}$-OEG$_{32}$. The sizes of both cross-linked and non-cross-linked PFH emulsions were approximately 180 nm in diameter by TEM and DLS (Figure S12). PFH emulsions both with and without cross-linking were heated to 56 and 70 °C and were observed by optical microscopy (Figure S13). It was found that the PFH emulsion after cross-linking did not show gas generation with heating up to 56 °C, proving that cross-linking of the polymeric shell increased emulsion stability when heated to the boiling point of the PFC. Moreover, this stabilizing effect was such that introduction of acoustic energy using a clinical ultrasound unit did not result in a phase transition at 37 °C (Figure S14). To test the limits, we confirmed the cross-linked PFH emulsions were broken at 70 °C with gas release observed upon heating to this higher temperature (Figure S13).

Once the chemistry was validated with the more easily handled PFH, we then switched to the low-bp PFP (bp 29 °C), for emulsification. DLS of the resulting emulsion after cross-linking showed an average diameter of approximately 250 nm, while that of the non-cross-linked emulsion was approximately 400 nm with a broader distribution (Figure S15). PFP emulsions with and

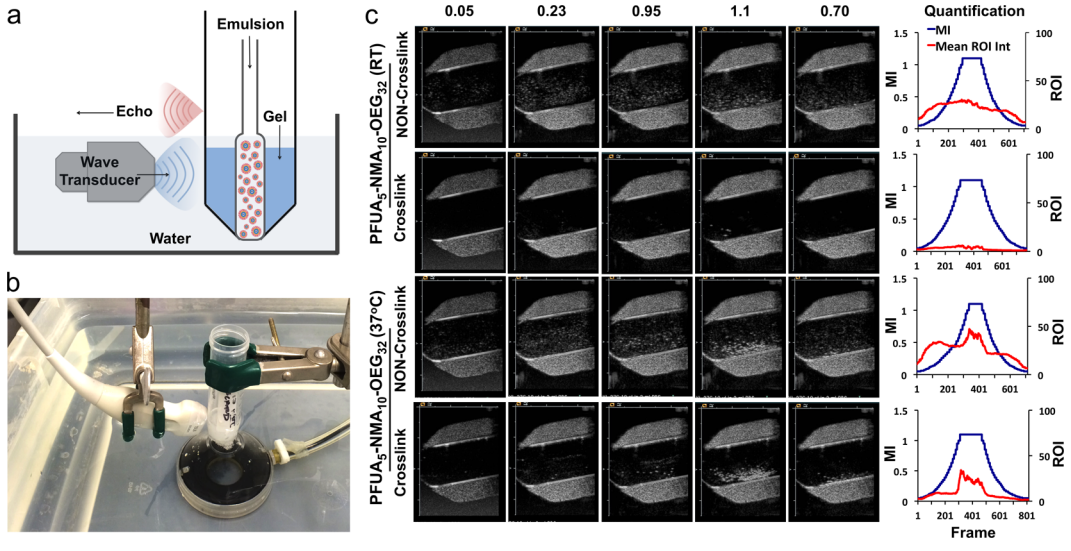

Figure 2. (a) Schematic diagram and (b) photograph of the ultrasound setup used for emulsion vaporization. An agarose gel containing 0.5% cellulose was used to hold the sample vial in place as well as to provide a standard scatterer. (c) Ultrasound images of PFP emulsions with PFUA$_5$-NMA$_{10}$-OEG$_{32}$ along with changes of ultrasound mechanical index (MI) at room temperature (RT) and physiological temperature (37 °C) respectively, and region of interest (ROI) intensity analysis of ultrasound signal intensity at the electronic focus of the transducer in one ultrasound test cycle. The blue line in each plot represents MI over time. The red line in each plot represents the response of the material with changing MI shown as mean ROI signal intensity.

DOI: 10.1021/jacs.6b08800
J. Am. Chem. Soc. 2017, 139, 15−18

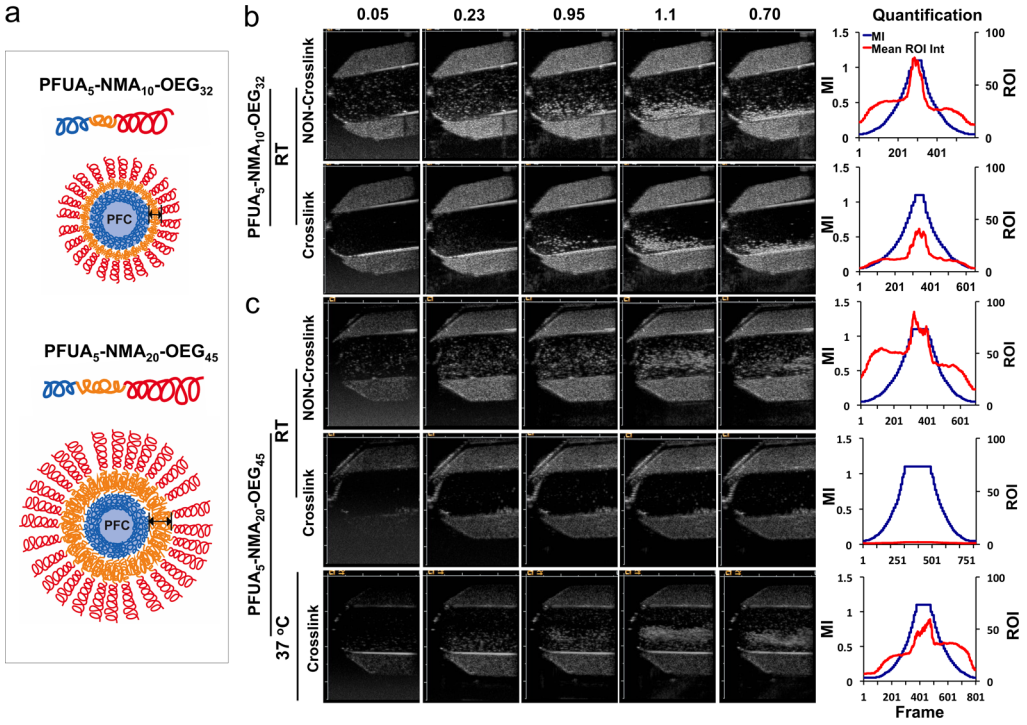

Figure 3. (a) Schematic diagram of PFB emulsions fabricated by $PFUA_5$-NMA_{10}-OEG_{32} and $PFUA_5$-NMA_{20}-OEG_{45}, respectively. (b) Ultrasound images of PFB emulsions fabricated by $PFUA_5$-NMA_{10}-OEG_{32}. (c) Ultrasound images of PFB emulsions fabricated by $PFUA_5$-NMA_{20}-OEG_{45} along with changes of ultrasound MI at room temperature (RT) and physiological temperature (37 °C) respectively, and region of interest (ROI) intensity analysis of ultrasound signal at the electronic focus of the transducer in one ultrasound test cycle. The blue line in each plot represents MI over time. The red line in each plot represents the response of the material with changing MI shown as mean ROI signal intensity.

without cross-linking were examined for contrast generation using a clinical diagnostic ultrasound machine (Figure 2). The output power of ultrasound exposure is proportional to the mechanical index (MI), with the maximum MI of diagnostic ultrasound approved by the Food and Drug Administration (FDA) being 1.9. To stay below the maximum ultrasound output power, we set the highest MI to 1.1 in our ultrasound tests. Ultrasound power was gradually increased from the lowest setting (−30 dB, MI = 0.05) to the highest (0 dB, MI = 1.1) and then cycled back to the lowest again at an average rate of 1 dB/s. We refer to this process as the "ultrasound test cycle", designed to determine the threshold for ADV as well as the amount of contrast generated at varying acoustic input energies. Once gas bubbles are triggered to form by ultrasound energy input, they appear as bright spots that increase with more gas bubbles released. Therefore, we quantified the bright spots in the test regions indicated as mean region of interest (ROI) intensity, plotted together with corresponding MI values over multiple frames (far right plots Figure 2). Without cross-linking, this emulsion was unstable at both ambient and physiological temperature (Figure 2c). That is, PFP liquid inside the non-cross-linked emulsion vaporized at the lowest ultrasound setting. By contrast, cross-linked PFP was stable at room temperature (near PFP bp) and no ADV was induced at any point during the ultrasound test cycle, suggesting the cross-links successfully stabilized PFP nanodroplets and prevented their phase transition at the highest ultrasound pressure used. However, when cross-linked PFP nanodroplets were heated to physiological temperature, ADV began at MI = 0.95, nearly at the maximal output of a clinical system in our defined ultrasound tests.

With an understanding of the behavior of PFP emulsions with and without cross-linking, we emulsified PFB (bp −1.7 °C) with $PFUA_5$-NMA_{10}-OEG_{32} to see whether cross-linking could afford stability to this highly volatile PFC when emulsified. At room temperature, the PFB emulsion without cross-linking was clearly unstable, with gas bubbles collecting along the container wall. Non-cross-linked PFB emulsions vaporized at even the lowest ultrasound exposure, and the cross-linked PFB emulsion vaporized at a very low pressure (MI = 0.23). We hypothesized that emulsifying PFB with a higher molecular weight polymer would afford greater stability to the cross-linked emulsion (Figure 3). Therefore, we synthesized $PFUA_5$-NMA_{20}-OEG_{45} a triblock copolymer with twice as many cross-linking units (Figure S16). The non-cross-linked PFB emulsion at ambient temperature vaporized continuously, even at the lowest possible ultrasound exposure, while cross-linking created a stable emulsion, which could not be vaporized even with the highest available ultrasound input (MI = 1.1). However, after increasing the test temperature to 37 °C, the cross-linked PFB emulsion started releasing gas bubbles at MI = 0.23 and underwent a burst release of PFB at MI = 1.1. By contrast, the non-cross-linked PFB-emulsion showed vaporization during the whole test cycle at 37 °C (Figure S17). Together, these data show that while the $PFUA_5$-NMA_{10}-OEG_{32} was able to stabilize PFH and PFP emulsions, the more volatile PFB emulsion required a new polymer, $PFUA_5$-NMA_{20}-OEG_{45}, providing twice as many cross-linking points.

To advance this cross-linkable polymer-stabilized PFC-emulsion concept to *in vivo* use in the future, we tested the stability of PFP emulsions over time, showing increased stability for cross-linked systems for both PFP and PFB formulations as determined by DLS (Figure S18). In addition, increases in size and dispersity were verified by DLS following ultrasound burst for both of these systems consistent with the transition from

DOI: 10.1021/jacs.6b08800
J. Am. Chem. Soc. 2017, 139, 15−18

droplet to gas phase PFC disrupting the initial structures (Figure S19). To test the materials for ultrasound response in more relevant biological fluids, we studied the PFP emulsion with polymer $PFUA_5$-NMA_{10}-OEG_{32} and PFB emulsion with the polymer $PFUA_5$-NMA_{20}-OEG_{45} in PBS with 55% Fetal Bovine Serum (FBS) at 37 °C (Figures S20 and S21). The cross-linked PFP-emulsions were again more stable in each case compared with the non-cross-linked versions. Notably, the PFP emulsion showed less gas release in serum at MI = 1.1 compared to when observed in PBS. This may be attributed to the increased viscosity of the fluid resulting in an increase in pressure on the surface of the PFP emulsion. Similarly, the cross-linked PFB emulsion was more stable than the non-cross-linked one, showing a release of vaporization at MI = 0.95 and a burst release at MI = 1.1. The cytotoxicity of both PFP and PFB emulsions were tested after incubating with HeLa cells for 24 h, respectively. Both non-cross-linked and cross-linked PFP and PFB emulsions indicated good biocompatibility at 0.1 μg/mL–0.1 mg/mL after 24 h of incubation.

In conclusion, we have formulated a UV-inducible thiol–ene click cross-linkable polymeric surfactant for encapsulation and stabilization of low boiling point PFCs. These polymers were assessed for their stabilizing properties and responsiveness to clinical ultrasound acoustic activation under room or physiological temperatures. With this system, it is possible to emulsify low-bp PFCs and provide stability. This is an important first step toward harnessing these triggerable contrast agents for eventual clinical applications as ADV agents, overcoming instability that currently leads to nonspecific or premature vaporization. Furthermore, this ROMP based polymeric system represents an easy and flexible way of tuning materials properties to account for different PFCs. Remarkably, PFB could be utilized in this manner with clinically relevant ultrasound, at physiological temperatures and in biological fluid despite having a boiling point of −1.7 °C.

■ ASSOCIATED CONTENT

Supporting Information

The Supporting Information is available free of charge on the ACS Publications website at DOI: 10.1021/jacs.6b08800.

Synthetic methods and characterization of compounds and polymers; TEM and DLS data for PFC emulsions, including optical microscopy images and ultrasound images (PDF)

■ AUTHOR INFORMATION

Corresponding Author

*ngianneschi@ucsd.edu

ORCID

Nathan C. Gianneschi: 0000-0001-9945-5475

Notes

The authors declare no competing financial interest.

■ ACKNOWLEDGMENTS

The authors acknowledge support of this work by the Army Research Office (W911NF-14-1-0169 and W911NF-15-1-0568). A.M.V. was supported by the NCI R25T institutional training grant 1R25CA153915-01 (Cancer Researchers in Nanotechnology (CRIN)) and T32 training grant NIH-NIBIB-T32-5T32EB005970 (Training Clinical Scientists in Radiological Imaging).

■ REFERENCES

(1) Huang, Y.; He, S.; Cao, W.; Cai, K.; Liang, X.-J. *Nanoscale* **2012**, *4*, 6135.
(2) Schutt, E. G.; Klein, D. H.; Mattrey, R. M.; Riess, J. G. *Angew. Chem., Int. Ed.* **2003**, *42*, 3218.
(3) Lindner, J. R. *Nat. Rev. Drug Discovery* **2004**, *3*, 527.
(4) Hernot, S.; Klibanov, A. L. *Adv. Drug Delivery Rev.* **2008**, *60*, 1153.
(5) Szíjjártó, C.; Rossi, S.; Waton, G.; Krafft, M. P. *Langmuir* **2012**, *28*, 1182.
(6) Matsunaga, T. O.; Sheeran, P. S.; Luois, S.; Streeter, J. E.; Mullin, L. B.; Banerjee, B.; Dayton, P. A. *Theranostics* **2012**, *2*, 1185.
(7) Rapoport, N. *Wiley Interdisciplinary Reviews: Nanomedicine and Nanobiotechnology* **2012**, *4*, 492.
(8) Mattrey, R. F.; Scheible, F. W.; Gosink, B. B.; Leopold, G. R.; Long, D. M.; Higgins, C. B. *Radiology* **1982**, *145*, 759.
(9) Mattrey, R. F.; Strich, G.; Shelton, R. E.; Gosink, B. B.; Leopold, G. R.; Lee, T.; Forsythe, J. *Radiology* **1987**, *163*, 339.
(10) Mattrey, R. F.; Wrigley, R.; Steinbach, G. C.; Schutt, E. G.; Evitts, D. P. *Invest. Radiol.* **1994**, *29*, S139.
(11) Mattrey, R. F.; Steinbach, G.; Lee, Y.; Wilkening, W.; Lazenby, J. *Acad. Radiol.* **1998**, *5*, S63.
(12) Cox, B.; Beard, P. *Nature* **2015**, *527*, 451.
(13) Zhou, Y.; Wang, Z.; Chen, Y.; Shen, H.; Luo, Z.; Li, A.; Wang, Q.; Ran, H.; Li, P.; Song, W. *Adv. Mater.* **2013**, *25*, 4123.
(14) Kennedy, J. E. *Nat. Rev. Cancer* **2005**, *5*, 321.
(15) Huynh, E.; Leung, B. Y.; Helfield, B. L.; Shakiba, M.; Gandier, J.-A.; Jin, C. S.; Master, E. R.; Wilson, B. C.; Goertz, D. E.; Zheng, G. *Nat. Nanotechnol.* **2015**, *10*, 325.
(16) Rossi, S.; Waton, G.; Krafft, M. P. *Langmuir* **2010**, *26*, 1649.
(17) Wilson, K.; Homan, K.; Emelianov, S. *Nat. Commun.* **2012**, *3*, 618.
(18) Rapoport, N.; Nam, K.-H.; Gupta, R.; Gao, Z.; Mohan, P.; Payne, A.; Todd, N.; Liu, X.; Kim, T.; Shea, J. *J. Controlled Release* **2011**, *153*, 4.
(19) Lentacker, I.; De Geest, B. G.; Vandenbroucke, R. E.; Peeters, L.; Demeester, J.; De Smedt, S. C.; Sanders, N. N. *Langmuir* **2006**, *22*, 7273.
(20) Niu, D.; Wang, X.; Li, Y.; Zheng, Y.; Li, F.; Chen, H.; Gu, J.; Zhao, W.; Shi, J. *Adv. Mater.* **2013**, *25*, 2686.
(21) Wang, X.; Chen, H.; Chen, Y.; Ma, M.; Zhang, K.; Li, F.; Zheng, Y.; Zeng, D.; Wang, Q.; Shi, J. *Adv. Mater.* **2012**, *24*, 785.
(22) Jia, X.; Cai, X.; Chen, Y.; Wang, S.; Xu, H.; Zhang, K.; Ma, M.; Wu, H.; Shi, J.; Chen, H. *ACS Appl. Mater. Interfaces* **2015**, *7*, 4579.
(23) Sirsi, S.; Borden, M. *Bubble Sci., Eng., Technol.* **2009**, *1*, 3.
(24) Sheeran, P. S.; Luois, S. H.; Mullin, L. B.; Matsunaga, T. O.; Dayton, P. A. *Biomaterials* **2012**, *33*, 3262.
(25) Wang, X.; Chen, H.; Zheng, Y.; Ma, M.; Chen, Y.; Zhang, K.; Zeng, D.; Shi, J. *Biomaterials* **2013**, *34*, 2057.
(26) Qin, S.; Caskey, C. F.; Ferrara, K. W. *Phys. Med. Biol.* **2009**, *54*, R27.
(27) De Jong, N.; Emmer, M.; Van Wamel, A.; Versluis, M. *Med. Biol. Eng. Comput.* **2009**, *47*, 861.
(28) Zhao, Y.-Z.; Du, L.-N.; Lu, C.-T.; Jin, Y.-G.; Ge, S.-P. *Int. J. Nanomed.* **2013**, *8*, 1621.
(29) Nakatsuka, M. A.; Mattrey, R. F.; Esener, S. C.; Cha, J. N.; Goodwin, A. P. *Adv. Mater.* **2012**, *24*, 6010.
(30) Jiang, G. J. *J. Appl. Polym. Sci.* **2009**, *114*, 3472.
(31) Hoyle, C. E.; Bowman, C. N. *Angew. Chem., Int. Ed.* **2010**, *49*, 1540.
(32) Thompson, M. P.; Randolph, L. M.; James, C. R.; Davalos, A. N.; Hahn, M. E.; Gianneschi, N. C. *Polym. Chem.* **2014**, *5*, 1954.
(33) Ku, T.-H.; Chien, M.-P.; Thompson, M. P.; Sinkovits, R. S.; Olson, N. H.; Baker, T. S.; Gianneschi, N. C. *J. Am. Chem. Soc.* **2011**, *133*, 8392.
(34) Bielawski, C. W.; Grubbs, R. H. *Prog. Polym. Sci.* **2007**, *32*, 1.
(35) Nishihara, M.; Imai, K.; Yokoyama, M. *Chem. Lett.* **2009**, *38*, 556.

DOI: 10.1021/jacs.6b08800
J. Am. Chem. Soc. 2017, 139, 15–18